Hot-corrosion of AISI 1020 steel in a molten NaCl/Na_2SO_4 eutectic at 700°C

Mohammad Badaruddin, Ahmad Yudi Eka Risano, Herry Wardono, and Dwi Asmi

Citation: **1788**, 030066 (2017); doi: 10.1063/1.4968319
View online: http://dx.doi.org/10.1063/1.4968319
View Table of Contents: http://aip.scitation.org/toc/apc/1788/1
Published by the American Institute of Physics

Hot-Corrosion of AISI 1020 Steel in a Molten NaCl/Na_2SO_4 Eutectic at 700°C

Mohammad Badaruddin[1, a)], Ahmad Yudi Eka Risano[1], Herry Wardono[1], and Dwi Asmi[2]

[1]Department of *Mechanical Engineering, Faculty of Engineering, University of Lampung*
[2]*Department of Physics, Faculty of Mathematics and Natural Sciences, University of Lampung*
Jalan Soemantri Brojonegoro No.1, Bandar Lampung 35145, Indonesia

[a)]Corresponding author: mbruddin@eng.unila.ac.id

Abstract. Hot-corrosion behavior and morphological development of AISI 1020 steel with 2 mg cm^{-2} mixtures of various NaCl/Na_2SO_4 ratios at 700°C were investigated by means of weight gain measurements, Optical Microscope (OM), X-ray diffraction (XRD), scanning electron microscopy (SEM), and energy dispersive X-ray spectroscopy (EDS). The weight gain kinetics of the steel with mixtures of salt deposits display a rapid growth rates, compared with the weight gain kinetics of AISI 1020 steel without salt deposit in dry air oxidation, and follow a steady-state parabolic law for 49 h. Chloridation and sulfidation produced by a molten NaCl/Na_2SO_4 on the steel induced hot-corrosion mechanism attack, and are responsible for the formation of thicker scale. The most severe corrosion takes place with the 70 wt.% NaCl mixtures in Na_2SO_4. The typical Fe_2O_3 whisker growth in outer part scale was attributed to the $FeCl_3$ volatilization. The formation of FeS in the innermost scale is more pronounced as the content of Na_2SO_4 in the mixture is increased.

INTRODUCTION

Engineering material components in the coal fire power plants such as a boiler, heat exchanger, and pressure vessel made from cold-rolled AISI 1020 steel, undergo hot-corrosion when the sodium chloride from the ocean breeze mixes with Na_2SO_4 from the fuel and deposits on hot-section components, leading to accelerating attack of the steel. Low-grade fuels with high concentrations of sulfur, vanadium, and sodium are often used in coal-fired power generation. Hot-corrosion induced in the material components of Fe-based alloys at the structural engineering exposed to an environment containing a mixture of the salt Na_2SO_4–NaCl [1,2], generates the serious problem. The existence of such corrosive condensation layer on the surface of steel leads to hot corrosion which can considerably reduce the service life of high-temperature components.

Studies of hot-corrosion induced by mixtures of NaCl/Na_2SO_4 had been focused on Fe- and Ni- base alloys [3−6]. The addition of 75 wt.% NaCl in Na_2SO_4 coatings can easily cause the degradation of protective Cr_2O_3 layers on the 310 stainless steel at 750°C and after hot corrosion of 24 h, a lot of salts penetrated into protective Cr_2O_3 layers and contacted with the matrix, causing significant sulfidation [5]. It has been reported that the friction welded low alloy steel AISI 4140 and stainless steel AISI 304 suffered accelerated corrosion in a molten salt environment of NaCl–50%Na_2SO_4 at 650°C and showed spalling/sputtering of the oxide scale [4]. The steel's performance in oxidizing environments is well established, but its behavior in corrosive environments, particularly those containing sulfidizing species and/or chlorides have not been studied extensively. Thus, the high-temperature behavior of AISI 1020 steel with NaCl and/or Na_2SO_4 deposits at the eutectic of NaCl/Na_2SO_4 melt was studied. Both corrosion kinetics evolution and morphological development are investigated by means of weight gain measurements, metallographic examination, and the identification of the corrosion products. The relationship between the corrosion morphology and composition of deposited salt layers is also explored.

International Conference on Engineering, Science and Nanotechnology 2016 (ICESNANO 2016)
AIP Conf. Proc. 1788, 030066-1–030066-9; doi: 10.1063/1.4968319
Published by AIP Publishing. 978-0-7354-1452-5/$30.00

EXPERIMENTAL PROCEDURE

Commercial cold-rolled AISI 1020 steel was used as experimental materials in this study. The chemical composition of the alloy is Fe–0.2C−0.05P−0.05S−0.5Mn (in wt.%). Rectangular specimens were cut into coupons with dimensions of 20 mm × 10 mm × 2 mm by a water-cooled cutting machine. Coupon specimens were ground by a precision polishing machine prior to corrosion tests. Specimens for hot corrosion tests were coated with five $NaCl/Na_2SO_4$ mixtures (100/0 wt.%, 30/70 wt.%, 50/50 wt.%, 70/30 wt.% and 0/100 wt.%, hereafter in wt.%) separately until a total weight of deposits salts reached by 2 mg cm^{-2}. An air gun was used to spray one of five saturated aqueous salt solutions to produce a coat of fine salt particles on the specimen surface after the water evaporated. The process was repeated until the dry salt particles were deposited up to the designed value. Control specimens of AISI 1020 steel were kept salt free in their as polished condition. Each specimen was put in an alumina crucible of 5 Ml size with a cup, and then exposed to 700°C for 1−49 h inbox furnace under a static air.

The corrosion products were analyzed by XRD using monochromatic CuKα radiation operated at 40 kV and 100 mA. XRD data were compared with JCPDS standard files to identify the various phases present. Characterization of the cross-sectional scales was carried out with OM, SEM, and EDS.

RESULTS AND DISCUSSION

High Temperature Corrosion Kinetics

The corrosion kinetics of specimens with and without salt deposits are depicted in Fig.1(a) as a plot of a weight gain per unit area (mg cm^{-2}) vs. function of oxidation time (h). This figure indicates that the weight gain kinetics under dry air oxidation in steady state condition shows a slow weight gain growth, whereas the salt deposits is a rapid weight- gain growth oxidation, while the kinetics with salt deposits all display a rapid weight-gain growth rate involved in the steady stage and after breakaway corrosion for 49 h. The alloy with 70% NaCl mixtures revealed the highest weight gain after corrosion for 49 h, followed by that with 100% Na_2SO_4 deposit. The weight gain data for all specimens with/without the salts deposits follow the parabolic law as shown in Fig. 1(a). The weight gain versus square root of oxidation time ($s^{1/2}$) plots are shown in Fig 1(b) to establish the kinetics rate for determining the parabolic rate constant (k_p) of the hot- corrosion of AISI 1020 steel by linear regression.

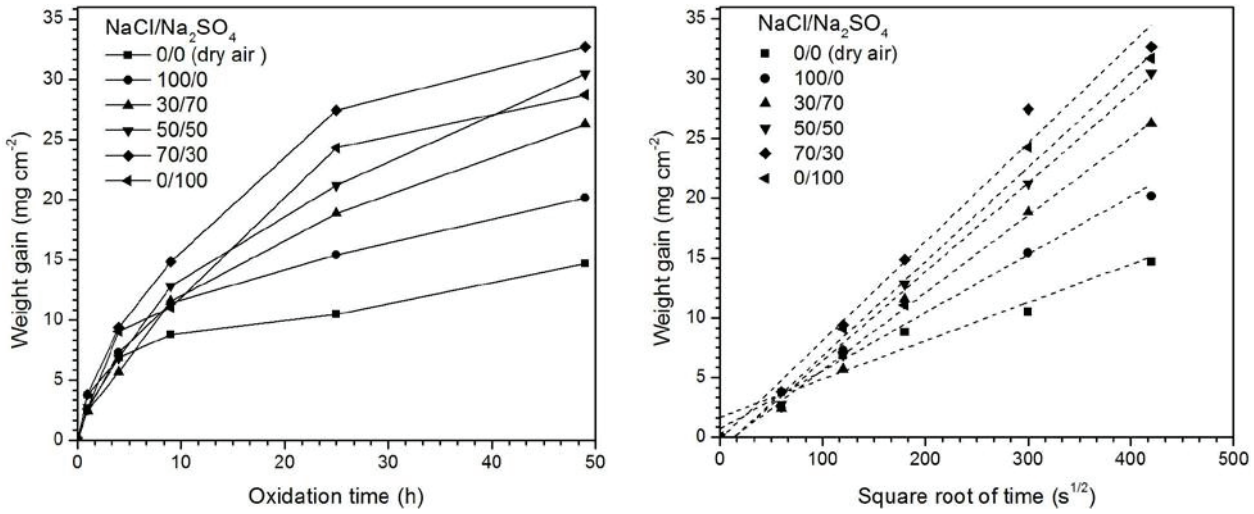

(a) (b)

FIGURE 1. (a) Oxidation kinetics and corrosion and (b) plot of weight gain vs. square root of oxidation time for AISI 1020 steel with/without $NaCl/Na_2SO_4$ mixtures in a static air at 700°C for 49 h

The calculated parabolic rate constants are summarized in Table 1. The corrosion rates increase by many factors of k_p with the addition of NaCl in the salt coatings. The corrosion rate of 100% NaCl coating is two factor of k_p than that of dry air oxidation. The highest of kp value is for the AISI 1020 steel with mixtures of 70 wt.% NaCl/30 wt.% Na_2SO_4.

TABLE 1. Parabolic rate constants for AISI 1020 steel with and without $NaCl/Na_2SO_4$ deposits oxidized at 700°C for 49 h

Composition ratios of $NaCl/Na_2SO_4$ (wt.%)	k_p ($g^2\ cm^{-4}\ s^{-1}$)
0/0	1.0259×10^{-9}
100/0	2.3746×10^{-9}
30/70	4.1977×10^{-9}
50/50	5.5473×10^{-9}
70/30	6.8327×10^{-9}
0/100	6.2378×10^{-9}

Macroscopic Observations

The surface appearance of the coupons after 9 h corrosion is shown in Fig. 2. In the case of mixtures of $NaCl/Na_2SO_4$ environment, the white color salt coating changed its color to brown with some small black spots observed whereas negligible reaction has taken place on the steel surface specimen. A thick scale with severe scale rumpling, cracking, and buckling is observed on a steel surface with $NaCl/Na_2SO_4$ deposits as shown in Fig. 2(a) to (d). The strongest corrosion is seen in low carbon steel with 70/30 wt.% ($NaCl/Na_2SO_4$) deposits as illustrated in Fig. 2(d). In addition, locally spelled oxides were identified on the surface of specimen with which remained in the molten salt as dispersed particles after specimen removal as depicted in Fig. 2(d). This can partly explain the weight loss shown in the corresponding weight gain curve as shown in Fig. 1(a). The surface of the specimen with Na_2SO_4 deposit shows the little buckling oxide on a macro scale. The dark gray color and texture of scale on the steel surface with Na_2SO_4 deposit was different from that on the steel surface with mixtures of $NaCl/Na_2SO_4$ as shown in Fig. 2(e).

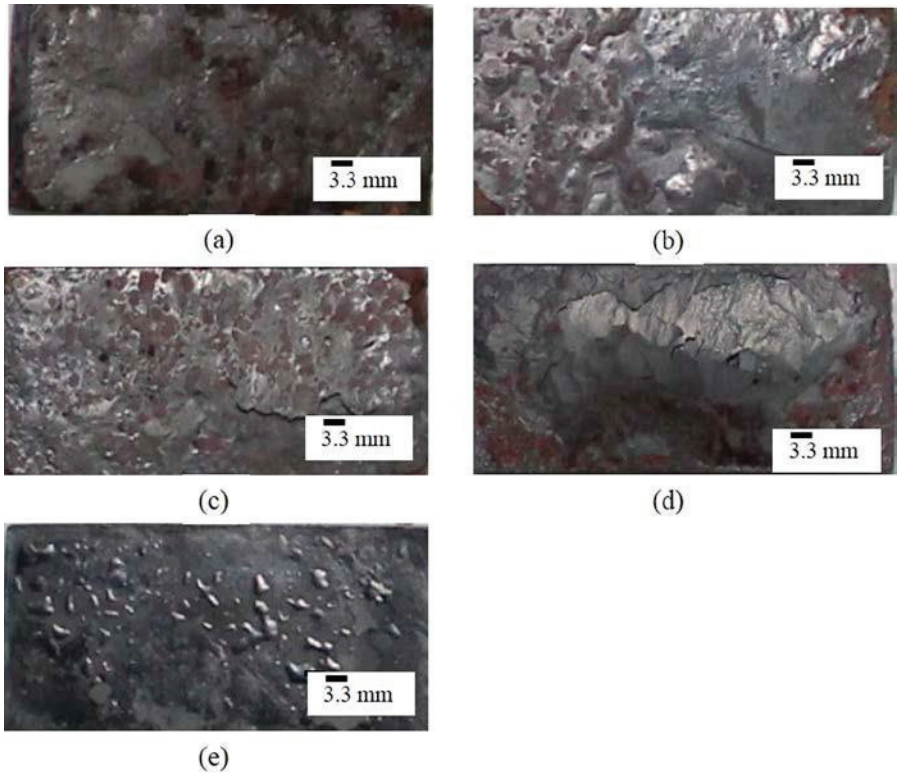

FIGURE 2. Magnification of macrographs of coupon specimens with different mixtures of $NaCl/Na_2SO_4$ deposits (a) 100/0, (b) 30/70, (c) 50/50, (d) 70/30, and (e) 0/100 after 9 h of hot-corrosion at 700 °C

Corrosion Morphology and Phase Constitutions

The oxidation behavior of carbon steel with NaCl, Na_2SO_4, and mixtures of both salt is relatively complicated and depends on temperature. The mixtures with compositions of 70%, 50%, and 30 % wt. NaCl were all completely melted at 700°C [7], indicating that Na_2SO_4 plays an important role as a source of acidic- and basic-fluxing, accelerating oxidation of the steel by hot-corrosion mechanism. During initial oxidation, low carbon steel exhibits accelerated oxidation owing to the reaction of oxide scale and NaCl/Na_2SO_4 coating. This initial stage is succeeded by a rapid oxidation rate, which is probably caused by reaction among iron, oxygen, and chloride on the steel substrate, forming Fe-oxide scale, leading to an increase in the corrosion kinetics. During rapid oxidation rate, the scale develops considerable porosity, as well as gaps between the oxide layers. Under these conditions, the oxidation rate is extremely sensitive to the amount of chlorine and sulfur gas in the atmosphere. Furthermore, oxidation dominates the entire corrosion reaction, despite the volatilization of the sodium chloride by elevating temperature or conversion to sodium sulfate by reaction with SO_3. As reported by Tsaur et al. [5], the presence of NaCl in the mixtures of NaCl/Na_2SO_4 could occur the most severe corrosion attack on high chromium content alloys. The addition of 75 wt.% NaCl in Na_2SO_4 coatings can easily crack of protective Cr_2O_3 layers and increase the amount of sulfur penetrated into the substrate, and then the corrosion of alloys was increased. The low-melting point of NaCl/Na_2SO_4 eutectic penetrates the oxide scale via the capillary effect [5] through pores and voids on the scale, and reacts with the steel substrate to cause oxidation. Regarding a side view of thermodynamics perspective, the final product of high-temperature corrosion is that with the lowest free energy in the system [8]. Comparison of the free energy of chloride, sulfide, and oxide indicates that the oxide is the corrosion product with the lowest free energy [5]. In the combined Cl–S–O atmosphere, oxide is the final constitution of the scale produced by hot-corrosion of AISI 1020 steel exposed to an environment containing Cl and S as shown in Fig. 3. In addition, all XRD analyses indicate that the constitutions of corrosion products are all iron oxides (Fig. 4).

The typical surface morphologies of specimens after high-temperature corrosion are shown in Fig. 3. All the scale formed by high-temperature corrosion has multi-layered structures with pores distributed on the scale in large numbers. The scales retain attachment on specimen surface with a small spallation (Fig. 3(a)). The scale morphologies as shown in Fig. 3(a) to (f) produced by a hot-corrosion of AISI 1020 steel with/without mixtures of NaCl/Na_2SO_4 at 700 ºC for 49 h, indicate that there are very dense pores existing on the surface of the main scale, as depicted in Fig. 3. In addition, the thickness of the scale is much greater than that of scale produced by a dry oxidation of AISI 1020 steel (Fig. 3(f)). The phase constitutions of the scales formed on the steel are regardless of hot-corrosion of AISI 1020 steel in mixtures of NaCl/Na_2SO_4 environment after 9 h of hot-corrosion at 700°C is shown in Fig. 4. Figure 4 shows the typical XRD patterns that the phase constitutions of scale formed from outside to inside are Fe_2O_3, Fe_3O_4, and $Fe_{1-X}O$. The outermost part of scale the marker “A” indicated contains Na_2SO_4, and the innermost part of scale the marker “B” indicated in Fig. 3(b) to (e) includes a very small amount of FeS. Figure 3a shows that the Fe_2O_3 scale produced by hot- corrosion of AISI 1020 steel with 100 wt.% NaCl deposit, is thicker than that of the Fe_2O_3 scale produced by hot- corrosion of AISI 1020 steel with mixtures of NaCl/Na_2SO_4 (Fig. 3b−e). This shows that the presence of higher composition of NaCl in Na_2SO_4 decreases a thickness of Fe_2O_3 scale after 49 h hot-corrosion. Distribution of iron oxides in the scale, as shown in Fig. 3(b) to (d), are the same as that obtained when the steel with 100 wt.% Na_2SO_4 subjected to hot-corrosion at 700 ºC for 49 h. Furthermore, the innermost part of the scale the marker “B” as shown in Fig. 3(b) has a large amount of FeS, and Na_2SO_4 can be found on the outermost part of the scale, as confirmed by XRD analysis (Fig. 4).

It was known that Fe_2O_3, Fe_3O_4, and $Fe_{1-X}O$ are the typical oxides formed on carbon steel when the steel was oxidized at the temperature higher than 570°C [9]. The constituents of scales showed the same results in this study, revealing that the corrosion of specimens was dominated by oxidation. The $Fe_{1-X}O$ is a p-type metal deficit semiconductor which contains large amount of defects [9], facilitating the iron ions to move outwards through the $Fe_{1-X}O$ layer. Thus it becomes a reason that the $Fe_{1-X}O$ layer is much thicker than the Fe_3O_4 and Fe_2O_3 layers. Besides that, in Fig. 3(e), a multi-layered structure is observed as a result from hot-corrosion of the steel with 100 wt.% Na_2SO_4 deposit, which may become a reason why the corrosion kinetics of the steel increases for 49 h of hot-corrosion at 700 ºC (Fig. 1(a)). On the contrary, the steel with 100 wt.% NaCl and mixtures of NaCl/Na_2SO_4 deposits show the lower corrosion kinetics is caused by vaporization Fe-chloride, as shown in Fig. 1(a). Thermodynamic calculations predict [5] that NaCl can be converted to Na_2SO_4 via a reaction with SO_2 in the atmosphere containing a high pressure of oxygen. Accordingly, the XRD analysis identifies Na_2SO_4, as indicated in Fig. 4. However, owing to the wetting effect through the formation of NaCl–Na_2SO_4 eutectic at 628°C [7], as well as the oxychloridation [5] of Fe in reaction with NaCl and oxygen to form Fe_2O_3, NaCl eventually may be consumed by volatilization of fused NaCl–Na_2SO_4 eutectic and oxychloridation.

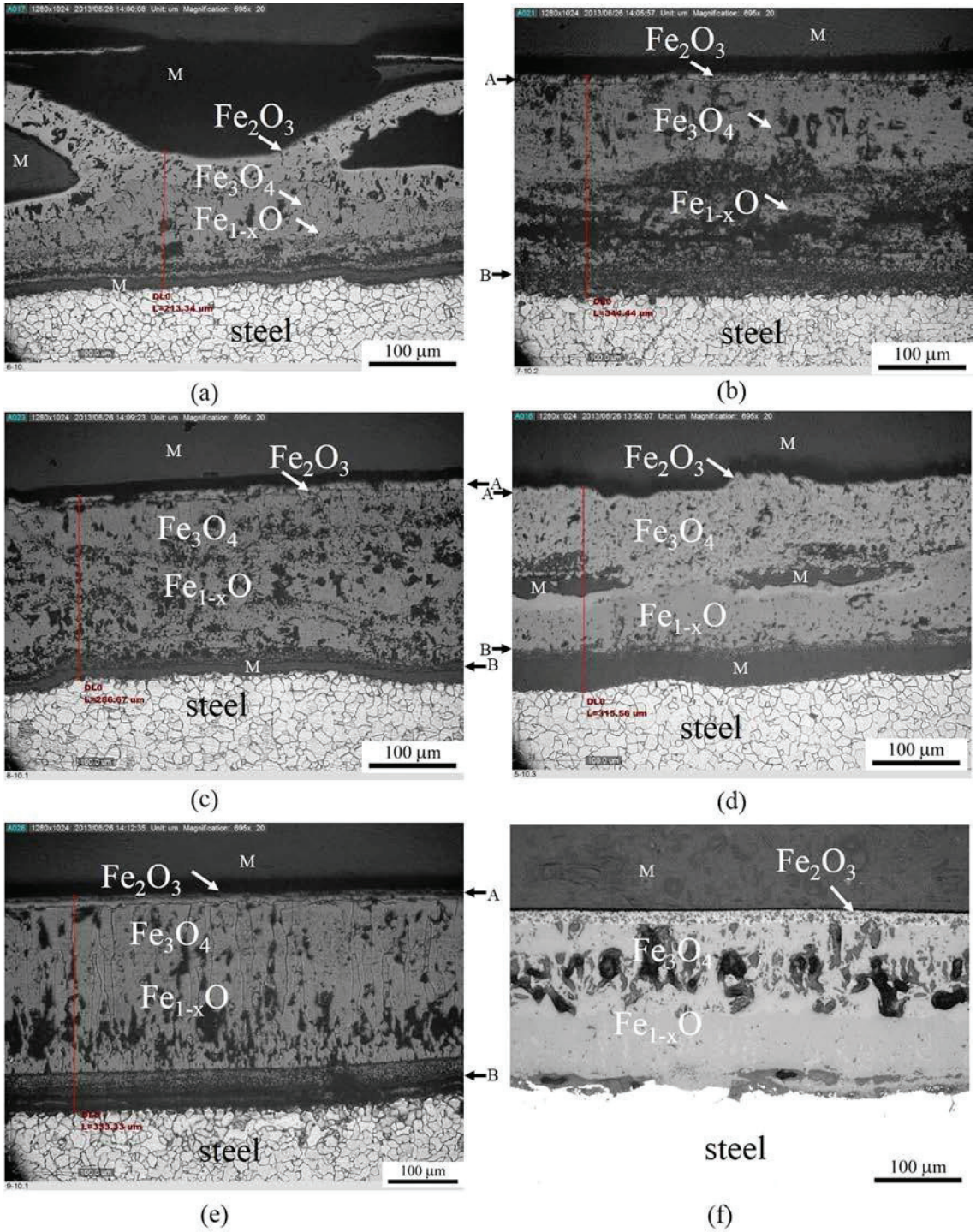

FIGURE 3. OM cross-sectional micrographs of AISI 1020 steel with and without NaCl/Na_2SO_4 coated exposed at 700°C for 49 h. (a) Pre-coated NaCl/Na_2SO_4 mixtures with the ratio of 100/0, (b) 70/30, (c) 50/50, (d) 30/70, (e) 0/100 and (f) dry air oxidation. (M) mounting; (A) outermost; (B) innermost.

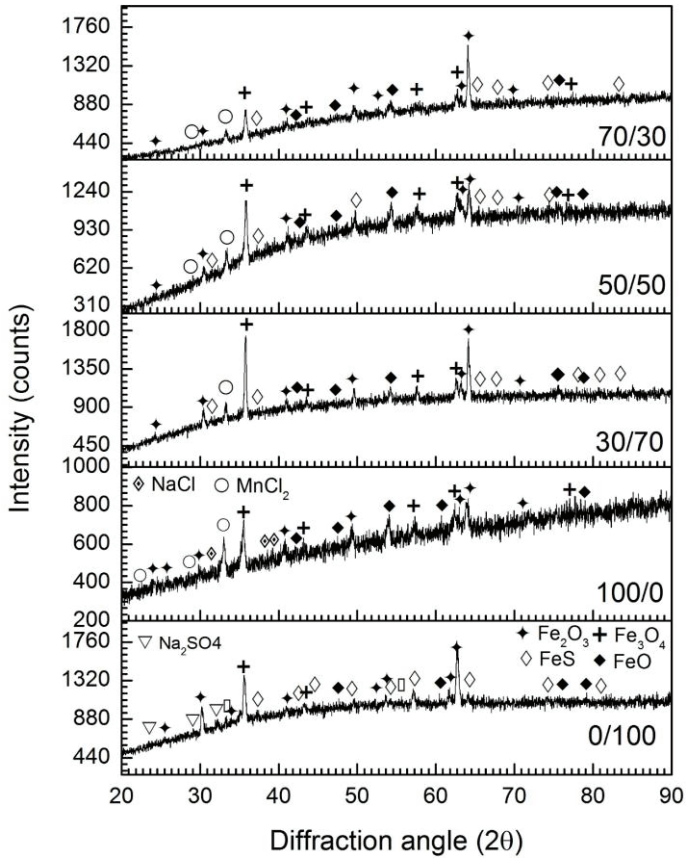

FIGURE 4. XRD analyses of corrosion products formed on AISI 1020 steel with a different ratios of $NaCl/Na_2SO_4$ deposits exposed at 700°C for 9 h

Figure 5(a) illustrates the surface morphology of AISI 1020 steel with 100 wt.% NaCl after hot corrosion of 49 h at 700°C. It can be seen that particles of corrosion products appear the Fe_2O_3 whiskers growth in outer part scale, and the corrosion products have formed films on the surface of AISI 1020 steel. Moreover, there are many white coarse particles growth with Fe_2O_3 whiskers growth. Figure 5(b) is the EDS spectrum confirmed that Mn detected in the scale after hot corrosion of 49 h at 700 °C. Moreover, the EDS quantitative analysis results in Fig. 5(c), show the composition of 3.18 at.% Mn detected in the scale. The outward diffusion of Mn^{2+} cations through the scale leads the coalescence of vacancies to form voids on the steel substrate [10]. As shown in Fig. 5(c), the high composition of Mn (at.%) on the scale indicates that the outward migration of manganese ion leads to an obvious formation of $MnCl_2$. It shows that not only $FeCl_3$ formed but also $MnCl_2$ formed during hot-corrosion of AISI 1020 steel with 100 wt.% NaCl deposit. Because the low melting temperature of $MnCl_2$ is 650°C [11], closing to the testing temperature in the present study. This result is evident with the XRD analysis in Fig. 4. Therefore, the white coarse particles formed together with the whiskers growth on the AISI 1020 steel substrate can be confirmed as the $MnCl_2$ particles. In addition, the low melting of $FeCl_3$ is 304°C [11], and can cause the $FeCl_3$ moving out via a crack path in the oxide scale to the high pressure of oxygen environment, and eventually react again with oxygen to form Fe_2O_3 and release Cl_2 gas again to the atmosphere. This is a reason why the Fe_2O_3 scale in 100 wt.% NaCl deposit on the steel has a thicker layer (Fig. 3(a)). This chlorine was liberated by the reaction between NaCl, O_2, and Fe which causes chloridation of AISI 1020 steel at 700ºC for 49 h. It shows that corrosion products are most iron oxides as shown in Fig. 4, which demonstrates that the types of corrosion products will not change during hot corrosion of 49 h. Furthermore, the products demonstrate that hot corrosion includes two processes, namely oxidation and chloridation.

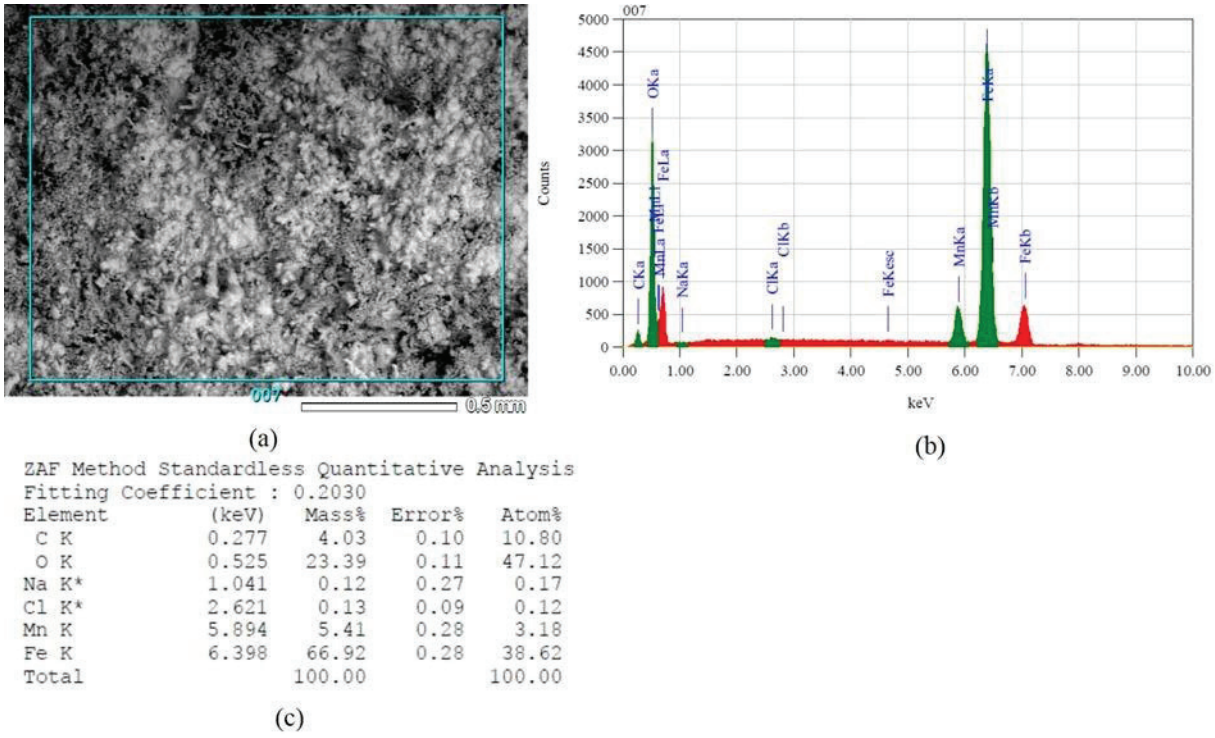

ZAF Method Standardless Quantitative Analysis
Fitting Coefficient : 0.2030

Element	(keV)	Mass%	Error%	Atom%
C K	0.277	4.03	0.10	10.80
O K	0.525	23.39	0.11	47.12
Na K*	1.041	0.12	0.27	0.17
Cl K*	2.621	0.13	0.09	0.12
Mn K	5.894	5.41	0.28	3.18
Fe K	6.398	66.92	0.28	38.62
Total		100.00		100.00

(c)

FIGURE 5. (a) SEM surface morphology of AISI 1020 steel with 100 wt.% NaCl deposit after hot corrosion of 49 h at 700 °C, (b) its EDS spectrum, and (c) EDS quantitative analyses in part (a)

Although the salt mixtures exist in a completely liquid phase at 700 °C, the fast evaporation characteristics of NaCl led to a residue of solid Na_2SO_4 on the specimen surface, as confirmed by XRD analysis (Fig. 4). Thus, in the initial stage oxidation, a molten NaCl could degrade scales on the steel surface. The scale structures formed by hot-corrosion of steel with 30/70 wt.% and 0/100 wt.% ($NaCl/Na_2SO_4$) are characterized by more wide-spread larger pores than in the structure formed by hot-corrosion of steel with 70/30 wt.% and 100/0 wt.% ($NaCl/Na_2SO_4$). The formation of iron sulfide at the innermost scale may be formed by a self-sustaining sulfidation reaction between Na_2SO_4/SO_3 formed between the scale and the substrate during hot-corrosion process. In a mixed salt environment, sulfur was incorporated into scale and proceeds to a sulfide formation in the steel substrate. Figure 6(a) depicts the surface morphology of AISI 1020 steel with mixtures of 70/30 wt.% $NaCl/Na_2SO_4$ after hot corrosion of 49 h at 700 °C. It is seen that corrosion products have formed density films on the surface and cracks emerge by the stress generated during films grow during hot-corrosion process. Some Fe_2O_3 whisker growth in the scale proves that the chloridation process induced hot- corrosion of the steel is the same with Fig. 5(a). Figure 6(b) is the EDS spectrum analysis after hot corrosion of 49 h at 700 °C. It reveals that Cl and S are detected in the surface scale. The low composition (at.%) of S in the scale (Fig. 6(c)) show that S penetrated into the scale via a crack path in the scale to form FeS, as confirmed by XRD results (Fig. 4). The large quantities of SO_2 molecules diffuse inwards from the salt/scale interface along micro-cracks or through the pores of the scale to the metal/scale interface [12]. In contrast, since the diffusion of Fe ion through the sulfide FeS is faster than through wustite [13], the sulfide forms a continuous layer in the innermost oxide, and scale growth rate increases rapidly. Evidently, the porous scale formed in a salt deposit promotes the inward diffusion of SO_2 and sulfide formation, as revealed in Fig. 3(b). Sulfide formation in the inner part of the scale also contributes to the rapid oxidation, as shown in Fig. 1a. In the atmosphere that contains Cl and S gas species, molecules of both species may reach the gap between the substrate and scale interface from the oxide scale via micro-cracks. However, when SO_3 diffuses from the atmosphere to the steel substrate, a thick layer of $Fe_{1-X}O$ develops, with many pores in the scale, which are means of access. This phenomenon facilitates the distribution of S. Therefore, a significant cluster of S exists as FeS on the inner side of the scale, as displayed in Fig. 3(b) and (e). Furthermore, Figure 6 also validates that hot corrosion includes the processes of oxidation, chloridation, and sulfidation.

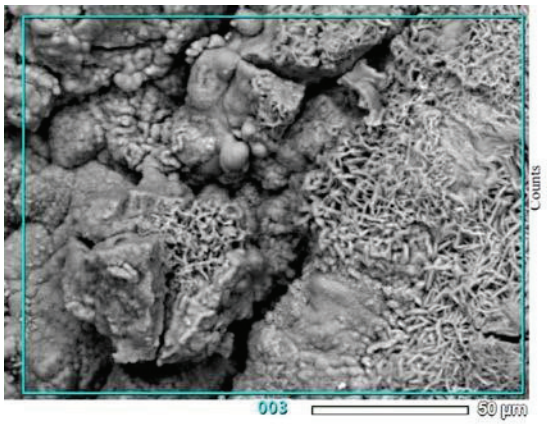

(a)

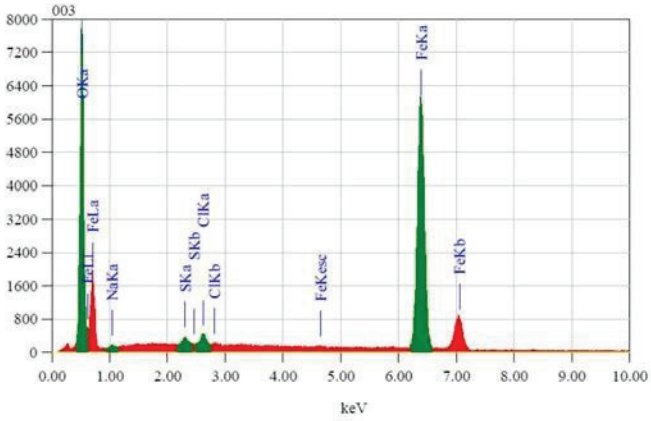

(b)

ZAF Method Standardless Quantitative Analysis
Fitting Coefficient : 0.1913

Element	(keV)	Mass%	Error%	Atom%
O K	0.525	36.04	0.10	65.81
Na K	1.041	0.47	0.28	0.59
S K	2.307	0.45	0.09	0.41
Cl K	2.621	0.70	0.10	0.57
Fe K	6.398	62.35	0.30	32.61
Total		100.00		100.00

(c)

FIGURE 6. (a) SEM surface morphology of AISI 1020 steel with mixtures of 70/30 wt.% ($NaCl/Na_2SO_4$) deposit after hot corrosion of 49 h at 700°C (b) its EDS spectrum, and (c) EDS quantitative analyses results in part (a)

CONCLUSIONS

The mixtures of 70% NaCl contained in a Na_2SO_4 can react rapidly and form Na_2SO_4–NaCl eutectics. The low-melting eutectic of Na_2SO_4–NaCl on steel surface for 49 h at 700ºC accelerates the corrosion kinetics of the steel. The mixtures with 70% NaCl showed the most severe corrosion on the steel substrate. Furthermore, the molten eutectic salt can become a capillary transport for penetrating Cl and S into iron-oxide scale. Fe_2O_3, Fe_3O_4, and $Fe_{1-x}O$ are main corrosion products on the AISI 1020 steel substrate. $MnCl_2$ formed with the Fe_2O_3 whisker growth in the scale is caused by the migration of manganese ions outward from the steel substrate. In addition, iron-sulfide (FeS) is found with increasing Na_2SO_4 content in the salt coating layer. The hot-corrosion of scale morphologies induced by increasing the composition of NaCl in Na_2SO_4 shows volatilation of iron-chlorides results, while the features of scale morphology of the steel produced by increasing the Na_2SO_4 content in the mixtures show a large amount of sulfides formation in innermost scale.

ACKNOWLEDGEMENT

The authors would like to thank to the Ministry of Research, Technology and Higher Education of the Republic of Indonesia for financial support via the Grant Research of the National Strategy under contract No.: 86/UN26/8/LPPM/2016.

REFERENCES

1. G. Liu, Y. Zhang, Z. Ni and R. Huang, Const. Build. Materials **115**, 1–5 (2016)
2. D. Lindberg, J. Niemi, M. Engblom, P. Yrjas, T. Lauren and M. Hupa, Fuel Process. Technology **141**, 285−298 (2016)
3. L. Zheng, Z. Maicang and D. Jianxin, Maters. Design **32**, 1981−1989 (2011)
4. N. Arivazhagan, S. Narayanan, S. Singh, S. Prakash and G. M. Reddy, Maters. Design **34**, 459–468 (2012)
5. C. C. Tsaur, J. C. Rock, C. J. Wang, Y. H. Su, Maters. Chem. Physics **89**, 445–453 (2005)
6. Y. Niu, F. Gesmundo, F. Viani, W. Wu, Oxid. Metals **42**, 265–284 (1994)
7. M.A. Clevinger, K.M. Kessel and C.G. Messina, in: H.M. Ondik (Ed.), *Phase Diagrams for Ceramists*, (The American Ceramic Society Inc., Columbus, Ohio, 1989), p.109
8. C. J. Wang and J. Y. Pan, Maters. Chem. Physics **82**, 965−973 (2003)
9. N. Birks, G. H. Meier and F. S. Pettit, *Introduction to the high-temperature oxidation of metals* 2nd Ed., (Cambridge University Press, Cambridge, 2006), pp. 83−86
10. C. J. Wang and Y. C. Chang, Maters. Chem. Physics **76**,151–161 (2002)
11. J. G. Speight, *Lange's Handbook of Chemistry* 16th Ed., (Mc. Graw-Hill, New York, 2005), pp. 38−142
12. V. Buscaglia, P. Nanni and C. Bottino, Corros. Science **30**, 327−349 (1990)
13. S. Mrowec and K. Przybylski, Oxid. Metals **23**, 107−139 (1985)